



## Towards the functionalization of the methine carbon of a sterically hindered tris(pyrazolyl)methane: is a radical pathway envisageable? Synthesis and structure of tetrakis(3,5-dimethylpyrazolyl)methane

Laurent Benisvy<sup>a,b</sup>, Riccardo Wanke<sup>a</sup>, Maxim L. Kuznetsov<sup>a</sup>, M. Fátima C. Guedes da Silva<sup>a,c</sup>, Armando J.L. Pombeiro<sup>a,\*</sup>

<sup>a</sup>Centro de Química Estrutural, Complexo I, Instituto Superior Técnico, TU Lisbon, Av. Rovisco Pais, 1049-001 Lisbon, Portugal

<sup>b</sup>Department of Chemistry, Bar-Ilan University, Ramat Gan 52900, Israel

<sup>c</sup>Universidade Lusófona de Humanidades e Tecnologias, ULHT Lisbon, Campo Grande 376, 1749-024 Lisbon, Portugal

### ARTICLE INFO

#### Article history:

Received 1 September 2009

Accepted 3 September 2009

Available online 6 September 2009

#### Keywords:

Tris(pyrazolyl)methane

Carbanion

Radical

Oxidation

DFT calculations

### ABSTRACT

Iodine oxidation, at  $-80\text{ }^{\circ}\text{C}$ , of the carbanion in  $[\{\text{C}(\text{pz}^{\text{Me}2})_3\}\text{Li}^+(\text{THF})]$  (**1**) (with  $\text{pz}^{\text{Me}2}$ =3,5-dimethylpyrazolyl) yields the C-centred radical in  $[\{\text{C}(\text{pz}^{\text{Me}2})_3\}\text{Li}^+(\text{THF})]^+$  (**1**<sup>+</sup>), which, upon warming to room temperature, produces the unprecedented tetrakis(3,5-dimethylpyrazolyl)methane  $\text{C}(\text{pz}^{\text{Me}2})_4$  (**3**), the X-ray structure of which revealing intramolecular C–H $\cdots\pi$  interactions between each 5-Me group and an adjacent pyrazolyl ring. Oxidation of the radical by  $\text{O}_2$  appears to lead to the novel ether  $(\text{pz}^{\text{Me}2})_3\text{C–O–C}(\text{pz}^{\text{Me}2})_3$  (**2**).

© 2009 Elsevier Ltd. All rights reserved.

### 1. Introduction

In contrast with the well developed chemistry of tris(pyrazolyl)hydroborates  $[\text{HB}(\text{pz}^{\text{R}})_3]^-$  [ $\text{pz}^{\text{R}}$ =pyrazolyl pz ( $\text{R}=\text{H}$ ) or substituted pyrazolyl ( $\text{R}\neq\text{H}$ )], which are among the most important six-electron *N*-donor ligands,<sup>1</sup> that of the isoelectronic and neutral tris(pyrazolyl)methane analogue  $\text{HC}(\text{pz}^{\text{R}})_3$  is still underdeveloped.<sup>2</sup> Nevertheless, in the last decade, a considerable synthetic progress has occurred, and various derivatives of tris- and bis(pyrazolyl)methane have been reported, and their coordination behaviour has been investigated.<sup>3,4</sup> Some of the complexes show interesting physicochemical properties with significance in fields spanning from catalysis to magnetic materials.<sup>4c</sup> It is believed that further synthetic development towards the functionalization of the central methine carbon atom would be greatly advantageous,<sup>4d</sup> as such changes to the backbone can dramatically influence the properties of the complexes, as well as permitting their attachment on a solid support.<sup>4e</sup>

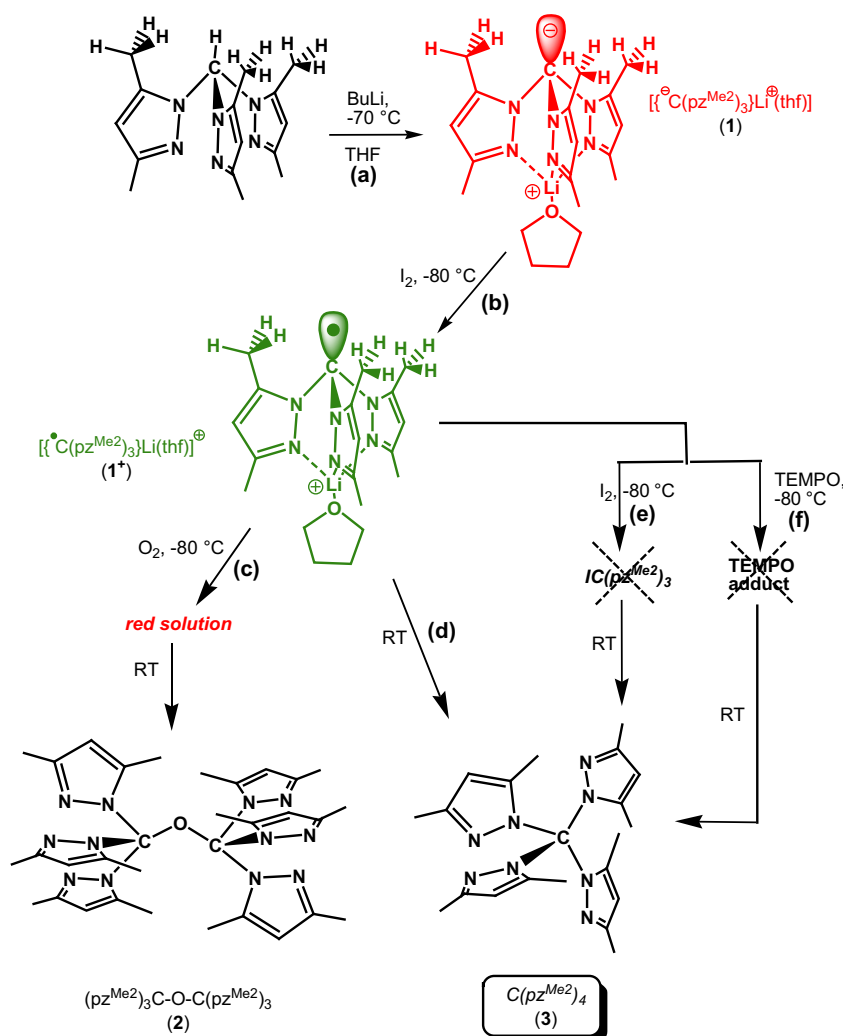
We have been interested in the functionalization of tris(pyrazolyl)methane  $\text{HC}(\text{pz})_3$  with a water soluble group such as sulfonate.<sup>5</sup> Substitution at the central methine carbon atom can be

achieved by reacting a suitable electrophile (e.g.,  $\text{RBr}$ , with  $\text{R}=\text{CH}_2\text{CH}_2\text{SO}_3^-$  for sulfonate derivatives; thiosylated aziridines for amine/ammonium derivatives) with the carbanion  $^-\text{C}(\text{pz})_3$  formed by deprotonation of  $\text{HC}(\text{pz})_3$ .<sup>4</sup> However, this method is unsuccessful for sterically hindered tris(pyrazolyl)methane compounds  $\text{HC}(\text{pz}^{\text{R}})_3$  ( $\text{R}\neq\text{H}$ ) and in order to explore new routes towards the functionalization of the central methine carbon, we have exploited in the current study the possibility of a radical pathway.

In particular, tris(3,5-dimethylpyrazolyl)methane  $\text{HC}(\text{pz}^{\text{Me}2})_3$  ( $\text{pz}^{\text{Me}2}$ =3,5-dimethylpyrazolyl) has currently attracted a great interest due to its specific electronic and steric properties, which give transition metal complexes unique properties.<sup>4c,d,f</sup> Interestingly, the corresponding red carbanion  $^-\text{C}(\text{pz}^{\text{Me}2})_3$  has been recently reported to display an unusual stability at room temperature what has even allowed the structural characterization of its lithium complex as  $[\{\text{C}(\text{pz}^{\text{Me}2})_3\}\text{Li}^+(\text{THF})]$  (**1**) (Scheme 1, reaction (a)).<sup>6</sup> This inertness of the carbanion has recently been further confirmed with the isolation and structural characterization of several complexes containing the  $\text{sp}^3$  hybridized carbanion,<sup>7a</sup> which acts as a six-electron  $\text{N}_3$ -donor face-capping ligand, e.g., in  $[\text{Mg}\{\text{C}(\text{pz}^{\text{Me}2})_3\}\text{Cl}]$ ,  $[\text{Mg}\{\text{C}(\text{pz}^{\text{Me}2})_3\}_2]$ ,  $[\text{Zn}\{\text{C}(\text{pz}^{\text{Me}2})_3\}\text{Me}]$ ,<sup>7b</sup>  $[\text{M}\{\text{C}(\text{pz}^{\text{Me}2})_3\}_2]$  (with  $\text{M}=\text{Fe}(\text{II})$ ,  $\text{Co}(\text{II})$ ),<sup>7c</sup>  $[\text{M}\{\text{C}(\text{pz}^{\text{Me}2})_3\}(\text{PPh}_3)]$  ( $\text{M}=\text{Cu}(\text{I})$ ,  $\text{Ag}(\text{I})$ )<sup>7d</sup> or in  $[\text{Ti}(\text{NBut})\{\text{C}(\text{pz}^{\text{Me}2})_3\}\text{Cl}(\text{THF})]$ .<sup>7e</sup> Interestingly, this carbanion appears to form stable carbon–metal bonds, e.g., with gold(I) as in  $[\text{Au}\{\text{C}(\text{pz}^{\text{Me}2})_3\}(\text{PPh}_3)]$ ,<sup>7d</sup> as well as its unsubstituted analogue in

\* Corresponding author. Fax: +351 21 846 4455.

E-mail address: pombeiro@ist.utl.pt (A.J.L. Pombeiro).



**Scheme 1.** Synthetic route to  $1^+$  and its derived products **2** and **3**.

the  $\text{W}(\text{Mo})/\text{Au}$  heterodimetallic compounds  $[\text{M}(\text{CR})(\text{CO})_2\text{Au}\{\text{C}(\text{pz})_3\}(\text{C}_6\text{F}_5)]$ .<sup>7f,g</sup>

However, the carbanion has been shown to be inert to electrophiles, thus preventing the incorporation of a substituent at the central carbon, what has been accounted for by the steric hindrance associated to the three methyl groups in position 5. The relative inertness of this carbanion led us to embark on the generation of its corresponding oxidized radical form  ${}^{\bullet}\text{C}(\text{pz}^{\text{Me}2})_3$  and the exploration of the reactivity of the latter.

Herein we report for the first time the generation and identification of the C-centred radical  ${}^{\bullet}\text{C}(\text{pz}^{\text{Me}2})_3$  as its  $\text{Li}^+$  salt,  $[\text{C}(\text{pz}^{\text{Me}2})_3\text{Li}(\text{THF})]^+$  ( $1^+$ ) and its chemical behaviour towards  $\text{O}_2$ , TEMPO (2,2,6,6-tetramethyl-1-piperidinyloxy) and  $\text{I}_2$ . The radical  $1^+$  reacts immediately with  $\text{O}_2$  to form the novel ether  $(\text{pz}^{\text{Me}2})_3\text{C}-\text{O}-\text{C}(\text{pz}^{\text{Me}2})_3$  (**2**). In the absence of  $\text{O}_2$ , we show that  $1^+$  undergoes decomposition yielding the unprecedented tetrakis(3,5-dimethylpyrazolyl)methane  $\text{C}(\text{pz}^{\text{Me}2})_4$  (**3**), which has been isolated and fully characterized, including by X-ray crystallography.

## 2. Results and discussion

### 2.1. Identification of the radical ${}^{\bullet}\text{C}(\text{pz}^{\text{Me}2})_3$

Upon reaction of tris(3,5-dimethylpyrazolyl)methane  $\text{HC}(\text{pz}^{\text{Me}2})_3$  with an equivalent amount of butyllithium at  $-70\text{ }^\circ\text{C}$  in THF, a red solution of  $[\text{C}(\text{pz}^{\text{Me}2})_3\text{Li}^+(\text{THF})]$  (**1**) was formed (Scheme 1,

reaction (a)). As expected from a previous report,<sup>6</sup> **1** was found to be stable upon warming to room temperature, and evaporation of the solvent gave a red-orange solid,  $^1\text{H}$  NMR data (in  $\text{THF}-d_8$ ) of which were identical to those reported<sup>6</sup> for **1** produced by using  $\text{MeLi}$  as a base. Importantly, the  $^1\text{H}$  NMR of the crude solid **1** did not show any significant signals of either  $\text{HC}(\text{pz}^{\text{Me}2})_3$  or other side products, indicating the clean quantitative formation of **1**. Therefore, **1** was used without any further purification.

Careful oxidation of **1**, at  $-80\text{ }^\circ\text{C}$  using 0.5 equiv of  $\text{I}_2$ ,<sup>†</sup> causes an instantaneous colour change to deep dark green, the formed species ( $1^+$ ) being stable for several hours only below  $-60\text{ }^\circ\text{C}$  under argon (Scheme 1, reaction (b)). The X-band EPR spectrum (Fig. S1 in Supplementary data) of a 1 mM THF frozen solution of  $1^+$ ,<sup>‡</sup> recorded at

<sup>†</sup> The use of a silver salt (e.g.,  $\text{Ag}[\text{BF}_4]$ ) as a one-electron oxidizing agent has proved to be unsuitable, as the only product identified, after purification, was the sandwich complex  $[\text{Ag}(\text{HC}(\text{pz}^{\text{Me}2})_3)_2][\text{BF}_4]$ , which was fully characterized including by X-ray crystallography [It is worth to note that although this compound is known,<sup>15</sup> there was no X-ray structural analysis with the tetrafluoroborate counter ion.] (see Supplementary data).

<sup>‡</sup> In this experiment, the anion was generated in a 1 mM concentration in THF; addition of 0.5 equiv of  $\text{I}_2$  produces the radical, which is present in  $\leq 1$  mM concentration (a suitable concentration for the detection of radical species by EPR spectroscopy) and the resulting solution was carefully transferred at  $-80\text{ }^\circ\text{C}$  to an EPR tube (kept under argon at  $-80\text{ }^\circ\text{C}$ ); the tube was then immediately cooled (and the solution frozen) in liquid nitrogen (77 K). No colour change has been detected during or after the transfer, indicating that the bright green colour characteristic of the radical remained.

95 K, exhibits an intense single isotropic signal at  $g=2.0026$  (with a peak-to-peak line width of ca. 15 G and no resolved hyperfine splitting) that is characteristic of that of an organic radical. The lack of any hyperfine structure in the EPR spectrum precludes any analysis of the spin density distribution within this species. However, since the line width of the signal is relatively narrow (ca. 15 G), any hyperfine splitting should be relatively small; this may indicate that the unpaired electron is not (or only to a limited extent; vide infra) localized on the *N*-pyrazole atoms, mostly residing on the central methine carbon. This is in accord with the (pseudo)tetrahedral conformation of the carbanion  ${}^{-}\text{C}(\text{pz}^{\text{Me}_2})_3$  in **1**, which lacks *p*-delocalization. Thus, we propose that the green species is the C-based radical  ${}^{\cdot}\text{C}(\text{pz}^{\text{Me}_2})_3$ , which presumably exists as the lithium complex  $\{[{}^{\cdot}\text{C}(\text{pz}^{\text{Me}_2})_3]\text{Li}(\text{THF})\}^+$  **1**<sup>+</sup>, formulated in a comparable manner to the parent  $\{[{}^{-}\text{C}(\text{pz}^{\text{Me}_2})_3]\text{Li}^+(\text{THF})\}$  **1**.

In order to corroborate this hypothesis, theoretical calculations of **1** and **1**<sup>+</sup> using the density functional theory (DFT) have been performed (see Experimental section). As shown in Table 1, the calculated bond lengths in **1** are in reasonable agreement with the corresponding X-ray structural data.<sup>6</sup> The maximum deviations of the theoretical and experimental parameters are 0.06 Å for the Li–O bond and 0.03 Å for the Li···C1 distance whereas the difference for the other bonds does not exceed 0.02 Å often falling within the 3σ interval of the X-ray data. The comparison of the equilibrium geometries of **1** and **1**<sup>+</sup> (Table 1) reveals that the oxidation mostly affects the geometry at the C1 carbon atom, namely (i) the N–C1–N angles significantly increase, (ii) the C1–N bonds and the distance between C1 and the plane formed by the N1, N2, and N3 atoms (*P*<sub>NNN</sub>) shorten, (iii) the angles between the pyrazolylic planes noticeably decrease and (iv) the dihedral angles NN···NN characterizing the mutual orientation of the pyrazolyl rings increase from 5.29–6.31° in **1** where all N–N bonds are almost parallel, to 28.70°–29.00° in **1**<sup>+</sup> where the pyrazolyl rings appear to be twisted relative to each other. These findings indicate a flattening of the tetrahedral geometry of the C1N<sub>3</sub> moiety upon oxidation. As a result, the C1···Li<sup>+</sup> distance becomes shorter by 0.117 Å despite the elongation of the Li–N bonds. Such a flattening is interpreted by the natural bond orbital (NBO) analysis (Table 2), which allows the determination of the orbital's hybridization type. This

**Table 1**  
Comparison of the experimental geometrical parameters reported<sup>6</sup> for **1** with those obtained by DFT calculations for **1** and **1**<sup>+</sup>

Bond distances (Å)	[ ${}^{-}\text{C}(\text{pz}^{\text{Me}_2})_3\text{Li}^+(\text{THF})$ ] ( <b>1</b> )			[ ${}^{\cdot}\text{C}(\text{pz}^{\text{Me}_2})_3\text{Li}(\text{THF})$ ] <sup>+</sup> ( <b>1</b> <sup>+</sup> )
	X-ray <sup>a</sup>	DFT <sub>calcd</sub> <sup>a</sup>	DFT <sub>calcd</sub> (this study)	DFT <sub>calcd</sub> (this study)
Li···C1	2.890	2.852	2.857	2.740
avLi–N	2.023	2.040	2.048	2.190
Li–O	1.908	1.983	1.972	1.905
avC1–N	1.448	1.449	1.448	1.403
avN–N	1.371	1.382	1.379	1.387
avC–N	1.326	1.331	1.333	1.330
avC–C	1.388	1.414	1.411	1.422
avC–C	1.364	1.384	1.385	1.376
avN–C	1.353	1.363	1.363	1.375
Distance C1··· <i>P</i> (NNN) (Å)	0.483	—	0.455	0.310
Angles	120.66	—	120.10	110.63
between	120.18	—	117.55	112.70
pz planes (°)	119.15	—	120.16	112.51
Angle N–C1–N	109.70	—	110.61	115.24
	109.47	—	—	115.33
	109.21	—	—	115.19
Dihedral angles	0.35	—	6.31	28.70
pz <sub>1</sub> NN–	1.56	—	5.29	29.00
pz <sub>2</sub> NN (°)	2.59	—	5.96	28.94

<sup>a</sup> Ref. 6.

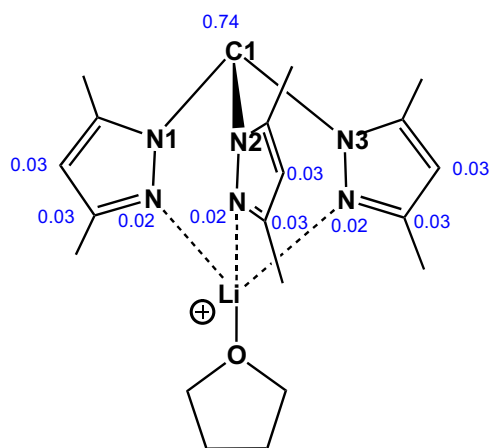
**Table 2**  
Results of the NBO analysis of **1** and **1**<sup>+</sup><sup>a</sup>

Bond orbital		<b>1</b>	<b>1</b> <sup>+</sup>
Lone pair or unpaired electron	Occ. η	1.81 s <sup>19.19</sup> p <sup>80.78</sup>	0.92 s <sup>10.87</sup> p <sup>89.13</sup>
C1–N1	Occ.	1.98	0.99
	C1 (%; η)	34.06; s <sup>26.90</sup> p <sup>72.93</sup>	36.81; s <sup>29.68</sup> p <sup>70.20</sup>
	N1 (%; η)	65.94; s <sup>36.24</sup> p <sup>63.73</sup>	63.19; s <sup>34.52</sup> p <sup>65.45</sup>
C1–N2	Occ.	1.98	0.99
	C1 (%; η)	34.08; s <sup>26.94</sup> p <sup>72.89</sup>	36.85; s <sup>29.76</sup> p <sup>70.13</sup>
	N1 (%; η)	65.92; s <sup>36.26</sup> p <sup>63.72</sup>	63.15; s <sup>34.44</sup> p <sup>65.53</sup>
C1–N3	Occ.	1.98	0.99
	C1 (%; η)	34.05; s <sup>26.94</sup> p <sup>72.89</sup>	36.83; s <sup>29.74</sup> p <sup>70.15</sup>
	N1 (%; η)	65.95; s <sup>36.27</sup> p <sup>63.71</sup>	63.17; s <sup>34.44</sup> p <sup>65.52</sup>

<sup>a</sup> The occupation, hybridization (η) and percent contribution of atomic orbitals to bond orbitals are indicated.

analysis demonstrates that the hybridization of the orbital of the C1 atom bearing the lone electron pair in **1** is sp<sup>4.2</sup> (where the superscript index indicates the p-character/s-character ratio of the hybrid orbital). The oxidation results in a significant increase of the relative contribution of p orbitals and the hybridization type in **1**<sup>+</sup> becomes sp<sup>8.2</sup>. By other words, the orbital of C1 bearing the unpaired electron in **1**<sup>+</sup> has predominantly p character.

The calculated atomic spin densities in **1**<sup>+</sup> (see Scheme 2) reveals that the unpaired electron is mainly localized at the methine carbon atom C1 (the spin density of 0.74). The remaining spin density is equally distributed onto the pyrazole rings (altogether ~0.09 for each ring). Thus, the low spin density on the pyrazole ring does not allow strong hyperfine coupling at N (*I*=1) or Pz-H (*I*=1/2), what justifies the relatively narrow EPR signal obtained for **1**<sup>+</sup>. Though the band width of the latter signal of 15 G suggests a certain amount of coupling, a decrease of the modulation amplitude (during EPR measurements) as low as 0.1 G did not allow to resolve these couplings. Since the three pyrazole rings are equivalent, the broadening of the signal may result from the hopping of the electron to pass from one ring to the other.



**Scheme 2.** Calculated spin density distribution in the optimized geometry of **1**<sup>+</sup>.

Thus, the results are convincing and consistent with our initial hypothesis based on the EPR study, both indicating that **1**<sup>+</sup> consists of the C-based radical  ${}^{\cdot}\text{C}(\text{pz}^{\text{Me}_2})_3$ , presumably coordinated to the lithium ion via the pyrazole *N*-atoms, being formulated as  $\{[{}^{\cdot}\text{C}(\text{pz}^{\text{Me}_2})_3]\text{Li}(\text{THF})\}^+$ .

## 2.2. Reactivity of ${}^{\cdot}\text{C}(\text{pz}^{\text{Me}_2})_3$

As a preliminary investigation of the reactivity of **1**<sup>+</sup> and in order to prove that substitution at the central carbon can be

achieved, freshly generated  $1^+$  was reacted with various reagents such as  $I_2$  (0.5 equiv),  $O_2$  (excess) and TEMPO (1 equiv) aiming the production of the iodo-compound  $IC(pz^{Me_2})_3$ , a C-peroxy species, and a TEMPO adduct, respectively.

Upon bubbling  $O_2$  through a THF solution of  $1^+$ , at  $-80^\circ C$ , the reaction mixture turned deep red within seconds (Scheme 1, reaction (c)). Subsequent work-up and purification led to the isolation of a single compound, **2**. The  $^1H$  NMR in  $CDCl_3$  of **2** exhibits three singlets at  $\delta$  5.83, 2.41 and 2.26 with 3:9:9 integrating ratios, respectively, which are typically assigned to the 4-H pyrazolyl atom, and the methyl groups at the 3 and 5 positions, correspondingly. Furthermore, positive electrospray shows two main peaks at 611 and 305, which may be attributed to  $[O\{C(pz^{Me_2})_3\}_2+H]^+$  and  $[O\{C(pz^{Me_2})_3\}_2]^{2+}$ , respectively. Thus, in the absence of X-ray structural data, we tentatively formulate this new species as the bis(tris(3,5-dimethylpyrazolyl)methane)ether compound  $(pz^{Me_2})_3C-O-C(pz^{Me_2})_3$ .

In all the other attempted reactions (Scheme 1, reactions (e) and (f), with  $I_2$  and TEMPO, respectively), three compounds were identified after work-up, i.e., free 3,5-dimethylpyrazole, the starting material  $HC(pz^{Me_2})_3$  and a new product, **3**. The same was observed when  $1^+$  was warmed up to room temperature without addition of any reagents (Scheme 1, reaction (d)), what indicates that **3** does not result from a radical condensation with the reagents but likely is a decomposition product of  $^{\cdot}C(pz^{Me_2})_3$  in  $1^+$ . The three products were separated by chromatography column over silica, and **3** was identified as the unprecedented tetrakis(3,5-dimethylpyrazolyl)methane,  $C(pz^{Me_2})_4$ , as indicated by  $^1H$ ,  $^{13}C$  NMR, IR, MS-EI and X-ray crystallography (see below). We suggest that a N-centred pyrazolyl radical  $^{\cdot}pz^{Me_2}$ , formed by decomposition of  $^{\cdot}C(pz^{Me_2})_3$ , couples with the parent  $^{\cdot}C(pz^{Me_2})_3$  to give  $C(pz^{Me_2})_4$ .

### 2.3. Characterization of $C(pz^{Me_2})_4$ (**3**)

The X-ray crystal structural analysis of **3** confirms its formulation as  $C(pz^{Me_2})_4$  without ambiguity (see Fig. 1) and thus demonstrates that substitution at the central methine carbon of  $HC(pz^{Me_2})_3$  can be achieved. Bond lengths (Å) and angles ( $^\circ$ ) in the structure of **3** are as expected for pyrazole compounds (see Table 3). However, a unique and striking feature of the structure is the presence of intramolecular C–H $\cdots\pi$  interactions specifically between each 5- $CH_3$  group and an adjacent pyrazolyl  $\pi$ -ring, as indicated in Figure 1. The distance between the C–H hydrogen and the centroid of the pyrazolyl ring lies in the 2.50–2.66 Å range, indicating a relatively strong non-covalent interaction (Table 2).<sup>7</sup>

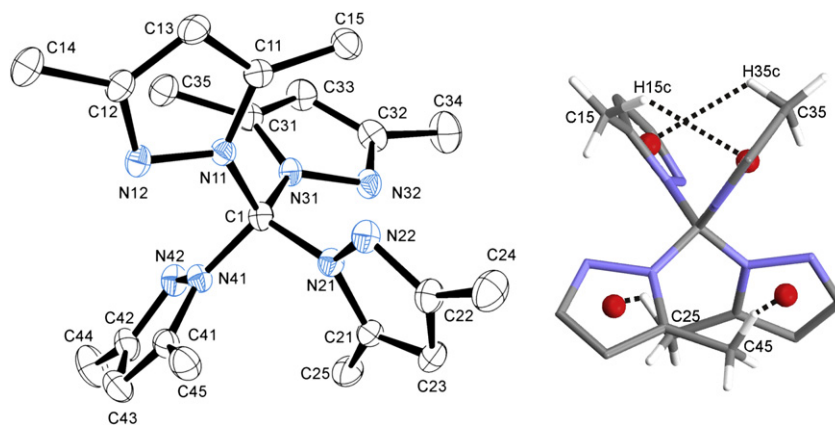


**Figure 1.** Representation of the molecular structure of  $C(pz^{Me_2})_4$ : (left) ORTEP plot shown at 50% probability (H-atoms have been omitted for clarity) and (right) representation of the intramolecular C–H $\cdots\pi$  interactions involving the 5- $CH_3$  group and an adjacent pyrazolyl  $\pi$ -ring (only the H-atoms of 5- $CH_3$  are shown and the 3- $CH_3$  groups have been omitted for clarity; the centroid of the pyrazole ring is represented as a red dot).

**Table 3**  
Selected bond lengths (Å) and angles ( $^\circ$ ) for compound **3**

(Å)	( $^\circ$ )		
C1N31	1.455(3)	N21–C1–N31	110.92(18)
C1N41	1.455(3)	N31–C1–N11	106.62(19)
C1N11	1.458(3)	N11–C1–N41	110.66(18)
C1N21	1.461(3)	N41–C1–N21	106.71(19)
		N31–C1–N41	110.73(19)
		N11–C1–N21	111.27(18)

The  $^1H$  NMR spectrum of **3** in  $CDCl_3$  exhibits the 3- $CH_3$  resonance at a chemical shift ( $\delta$  2.1) that is close to that ( $\delta$  2.2) of  $HC(pz^{Me_2})_3$ , but the resonance of the 5- $CH_3$  ( $\delta$  1.6) is unusually shifted to a lower frequency relatively to the corresponding one ( $\delta$  2.0) of  $HC(pz^{Me_2})_3$ . These observations may be indicative<sup>8,9</sup> of a significant magnetic effect exerted by the pyrazole rings (presumably via a ring current mechanism) on the 5- $CH_3$  protons, and may signify that the C–H $\cdots\pi$  interactions are retained in solution. It is noteworthy that the 1.6 ppm signal appears to be independent of the dilution factor (1:10:100) in various solvents such as  $CDCl_3$ ,  $CD_3OD$  and acetone- $d_6$ . Moreover, lowering the temperature to  $-60^\circ C$  did not induce any significant change either in the resolution or in the position this resonance (see Experimental section).

### 3. Conclusions

Whilst the recently reported<sup>6,7</sup> stable anion in  $[^{-}C(pz^{Me_2})_3] Li^+(THF)$  (**1**) has been shown to be inert to electrophilic attack, thus preventing the incorporation of a substituent at the central carbon atom, we herein have produced, for the first time, the corresponding C-centred radical  $^{\cdot}C(pz^{Me_2})_3$  which, in contrast, is highly reactive at low temperature. We have shown that this radical decomposes to form the unprecedented tetrakis-substituted methane  $C(pz^{Me_2})_4$ , which has been isolated and fully characterized including by X-ray crystallography. In spite of the bulkiness of its close four  $pz^{Me_2}$  groups,  $C(pz^{Me_2})_4$  is remarkably stable, being stabilized by intramolecular C–H $\cdots\pi$  interactions between each 5- $CH_3$  group and the pyrazolyl ring of an adjacent  $pz^{Me_2}$  moiety.  $C(pz^{Me_2})_4$  is of a potential significance as a novel  $N_4$  pro-ligand for assembling metal units e.g., towards the construction of polyfunctional coordination polymers. We are studying its coordination behaviour with various transition metal ions.

Moreover, the radical  $^{\cdot}C(pz^{Me_2})_3$  is oxidized by  $O_2$  to yield conceivably the ether function, i.e.,  $(pz^{Me_2})_3C-O-C(pz^{Me_2})_3$ .

These preliminary studies have demonstrated that substitution (functionalization) at the methine carbon of  $HC(pz^{Me_2})_3$  is feasible,

despite the steric hindrance imposed by the methyl groups, via a radical pathway involving the  $\cdot\text{C}(\text{pz}^{\text{Me}_2})_3$  radical. However, in order to reach general applicability to different substituents, a careful control of the reaction will be required to compete favourably with the formation of  $\text{C}(\text{pz}^{\text{Me}_2})_4$ . Hence, we are currently further investigating this radical path towards the functionalization of the central methine carbon.

## 4. Experimental section

### 4.1. General materials and experimental procedures

All syntheses and handling were carried out under an atmosphere of argon, using carefully Schlenk techniques for air sensitive chemistry. All solvents were dried by standard methods, degassed and distilled prior to use. All reagents were purchased from Aldrich and used without further purification. Tris(3,5-dimethylpyrazolyl)methane was synthesized in accordance with literature methods.<sup>4a</sup> Infrared spectra ( $4000\text{--}400\text{ cm}^{-1}$ ) were recorded on a BIO-RAD FTS 3000MX instrument in KBr pellets.  $^1\text{H}$ ,  $^{13}\text{C}$  and NMR spectra were measured on Bruker 300 and 400 UltraShield™ spectrometers at ambient and low temperatures.  $^1\text{H}$  and  $^{13}\text{C}$  chemical shifts  $\delta$  are expressed in parts per million relative to  $\text{Si}(\text{Me})_4$ . EPR analysis has been carried out in a Bruker ESP 300E spectrometer with an A-500 RF power amplifier. The experiments were collected at 95 K with the following parameters: centre field: 3343.56; modulation frequency: 100 KHz; modulation amplitude: 0.1 Gpp; receiver gain:  $4 \times 10^{-4}$ ; conversion time: 20 ms; time constant: 20 ms; ST: 42 s.

### 4.2. Computational details

The full geometry optimization of **1** and **1**<sup>+</sup> has been carried out in Cartesian coordinates at the DFT level of theory using the Gaussian 98<sup>10</sup> package. The calculations have been performed using Becke's three-parameter hybrid exchange functional<sup>11</sup> in combination with the gradient-corrected correlation functional of Lee et al.<sup>12</sup> (B3LYP) and the 6-31G\* basis set. Restricted approximations for the structure with closed electron shells and unrestricted methods for the structure with open electron shells have been employed. Symmetry operations were not applied. The Hessian matrix was calculated analytically to prove the location of correct minimum (no imaginary frequencies were found). The hybridization of atomic orbitals has been calculated using the natural bond orbital (NBO) partitioning scheme.<sup>13</sup> The experimental X-ray geometry of **1** was taken as a basis for the initial geometry of the optimization processes.

### 4.3. Synthesis of tetrakis(3,5-dimethylpyrazolyl)methane, $\text{C}(\text{pz}^{\text{Me}_2})_4$ ( $\text{pz}^{\text{Me}_2} = 3,5\text{-dimethylpyrazole}$ )

A 1.6 M solution of butyllithium (7.24 mL, 11.58 mmol, 1.15 equiv) in cyclohexane was added dropwise to tris(3,5-dimethylpyrazolyl)methane (3.00 g, 10.08 mmol, 1 equiv) in dry THF (100 mL) at  $-70\text{ }^\circ\text{C}$ . The solution turned orange-red and was stirred for 20 min at  $-60\text{ }^\circ\text{C}$ , then cooled down to  $-80\text{ }^\circ\text{C}$ . A solution of  $\text{I}_2$  (1.28 g, 5.03 mmol, 0.5 equiv) in dry THF (50 mL) was added dropwise to the red mixture under vigorous stirring at  $-80\text{ }^\circ\text{C}$ , causing a drastic colour change to deep intense green. The reaction mixture was stirred for a further 10 min at  $-80\text{ }^\circ\text{C}$ , and then allowed to warm to room temperature in 3 h; during this time the solution turned gradually to brown/yellow and a pale brown solid precipitate formed. The solvent was evaporated from the mixture to yield a brown solid. This was dissolved in  $\text{CH}_2\text{Cl}_2$  (40 mL) and the solution was washed with water ( $2 \times 20\text{ mL}$ ), dried over  $\text{Na}_2\text{SO}_4$ , filtered and evaporated, yielding a brown solid. The residue was

rapidly purified by flash chromatography passing through a silica column (100% pentane as eluent). The product was isolated as a white crystalline solid in 27% yield with respect to  $\text{HC}(\text{pz}^{\text{Me}_2})_3$ . Slow evaporation of a chloroform solution over 2 days yielded single crystals of  $\text{C}(\text{pz}^{\text{Me}_2})_4$  that were suitable for X-ray crystallography analysis.  $\text{C}_{21}\text{H}_{28}\text{N}_8$ : 392.5. IR (KBr): 3102 (m), 2961, 2926 (br s, CH), 1568 (vs,  $\nu_{\text{C}=\text{N}}$ ), 1413 (s), 1243 (vs, br), 924 (vs), 899 (vs), 793 (s), 758 (s)  $\text{cm}^{-1}$ . MS-EI  $m/z$ : 297  $[\text{C}(\text{pz}^{\text{Me}_2})_3]^+$ , 415  $[\text{C}(\text{pz}^{\text{Me}_2})_4 + \text{Na}]^+$ .  $^1\text{H}$  NMR (400 MHz,  $\text{CDCl}_3$ , 298 K): 5.93 (s, 4H, 4-H (pz)), 2.14 (s, 12H, 3-H<sub>3</sub>C (pz)), 1.67 (s, 12H, 5-H<sub>3</sub>C (pz)).  $^1\text{H}$  NMR (400 MHz, acetone- $d_6$ , 298 K): 6.00 (s, 4H, 4-H (pz)), 2.08 (s, 12H, 3-H<sub>3</sub>C (pz)), 1.64 (s, 12H, 5-H<sub>3</sub>C (pz)).  $^1\text{H}$  NMR (400 MHz, MeOD, 298 K): 6.14 (s, 4H, 4-H (pz)), 2.12 (s, 12H, 3-H<sub>3</sub>C (pz)), 1.64 (s, 12H, 5-H<sub>3</sub>C (pz)).  $^1\text{H}$  NMR (400 MHz,  $\text{CDCl}_3$ , 213 K): 5.97 (s, 4H, 4-H (pz)), 2.14 (s, 12H, 3-H<sub>3</sub>C (pz)), 1.62 (s, 12H, 5-H<sub>3</sub>C (pz)).  $^1\text{H}$  NMR (400 MHz, acetone- $d_6$ , 213 K): 6.06 (s, 4H, 4-H (pz)), 2.05 (s, 12H, 3-H<sub>3</sub>C (pz)), 1.58 (s, 12H, 5-H<sub>3</sub>C (pz)).  $^{13}\text{C}$  NMR (100 MHz,  $\text{CDCl}_3$ , 298 K): 147.21 (3-C (pz)), 144.67 (5-C (pz)), 109.22 (4-C (pz)), 97.98 ( $\text{C}(\text{pz}^{\text{Me}_2})_4$ ), 14.16 (3-CH<sub>3</sub> (pz)), 11.94 (5-CH<sub>3</sub> (pz)).

### 4.4. Synthesis of $[(\text{pz}^{\text{Me}_2})_3\text{C}-\text{O}-\text{C}(\text{pz}^{\text{Me}_2})_3]$ ( $\text{pz}^{\text{Me}_2} = 3,5\text{-dimethylpyrazolyl}$ )

A 1.6 M solution of butyllithium (230  $\mu\text{L}$ , 0.37 mmol, 1.1 equiv) in cyclohexane was added dropwise to tris(3,5-dimethylpyrazolyl)methane  $\text{HC}(\text{pz}^{\text{Me}_2})_3$  (100 g, 0.34 mmol, 1.0 equiv) in dry THF (10 mL) at  $-70\text{ }^\circ\text{C}$ . The solution was stirred for 1 h at  $-60\text{ }^\circ\text{C}$ , then cooled down to  $-90\text{ }^\circ\text{C}$  and a THF solution (2 mL) of  $\text{I}_2$  (43 mg, 0.17 mmol, 0.5 equiv) was added dropwise, via a cannula; the colour turned immediately to dark intense green and the mixture was kept stirred under argon atmosphere at  $-90\text{ }^\circ\text{C}$ . After the addition,  $\text{O}_2$  was bubbled through the solution, which turned instantaneously to deep red. The mixture was stirred at  $-90\text{ }^\circ\text{C}$  for 20 min and stored at  $-80\text{ }^\circ\text{C}$  overnight in a deep freezer. The reaction mixture was then allowed to warm to room temperature and the final solution (brown/red) was evaporated to give a brown solid. The product was purified by flash chromatography (acetone/pentane) to give a pale brown powder in 33% yield.  $^1\text{H}$  NMR (400 MHz,  $\text{CDCl}_3$ ): 5.83 (s, 3H, 4-H (pz)), 2.41 (br, 18H, 3-H<sub>3</sub>C (pz)), 2.26 (s, 18H, 5-H<sub>3</sub>C (pz)). MS-EI  $m/z$ : 611  $[\text{O}(\text{C}(\text{pz}^{\text{Me}_2})_3) + \text{H}]^+$ , 305  $[\text{O}(\text{C}(\text{pz}^{\text{Me}_2})_3)]^{2+}$ .

### 4.5. Crystal data

Intensity data were collected using a Bruker AXS-KAPPA APEX II diffractometer with graphite monochromated Mo  $K\alpha$  radiation. Data were collected at 150 K using omega scans of  $0.5^\circ$  per frame and a full sphere of data was obtained. Cell parameters were retrieved using Bruker SMART software and refined using Bruker SAINT on all the observed reflections. Absorption corrections were applied using SADABS. The structures were solved by direct methods by using the SHELXS-97 package<sup>14a</sup> and refined with SHELXL-97.<sup>14b</sup> Calculations were performed using the WinGX System-Version 1.80.03.<sup>14c</sup>

Compound  $\text{C}(\text{pz}^{\text{Me}_2})_4$ :  $\text{C}_{21}\text{H}_{28}\text{N}_8$ ,  $M = 392.51$ , triclinic, space group  $P-1$  (No. 2),  $a = 8.7193(8)$ ,  $b = 10.1915(12)$ ,  $c = 12.5175(12)$  Å,  $\alpha = 78.152(7)^\circ$ ,  $\beta = 84.766(5)^\circ$ ,  $\gamma = 69.968(6)^\circ$ ,  $U = 1022.52(19)$  Å<sup>3</sup>,  $Z = 2$ ,  $\mu(\text{Mo } K\alpha) = 0.081\text{ mm}^{-1}$ . All hydrogens were inserted in calculated positions. Least square refinement with anisotropic thermal motion parameters for all the non-hydrogen atoms and isotropic for the remaining atoms gave  $R_1 = 0.0558$  [ $I > 2\sigma(I)$ ];  $wR_2 = 0.1496$  (all data)]. The maximum and minimum peaks in the final difference electron density map are of 0.328 and  $-0.235\text{ e } \text{Å}^{-3}$ . CCDC 746012 and 746013 contain the supplementary crystallographic data for this paper. These data can be obtained free of charge from The

Cambridge Crystallographic Data Centre via [www.ccdc.cam.ac.uk/data\\_request/cif](http://www.ccdc.cam.ac.uk/data_request/cif).

## Acknowledgements

This work has been partially supported by the Foundation for Science and Technology (FCT), and its POCI 2010 programmes (FEDER funded), grant SFRH/BD/23187/2005 (R.W.), as well as by the Human Resources and Mobility Marie Curie Research Training Network (AQUACHEM project, CMTN-CT-2003-503864). L.B. thanks the EU for the provision of an ER fellowship within this project. M.L.K. is grateful to the FCT and IST for a research contract within the Ciência 2007 scientific programme.

## Supplementary data

Supplementary data associated with this article can be found in online version, at [doi:10.1016/j.tet.2009.09.006](https://doi.org/10.1016/j.tet.2009.09.006).

## References and notes

- (a) Trofimenko, S. *J. Am. Chem. Soc.* **1966**, *88*, 1842–1844; (b) Trofimenko, S. *Chem. Rev.* **1993**, *93*, 943–980; (c) Trofimenko, S. *Scorpionates: The Coordination Chemistry of Polypyrazolylborates Ligands*; Imperial College: London, 1999.
- Reger, D. L.; Grattan, T. C. *Synthesis* **2003**, 350–356.
- (a) Pettinari, C.; Pettinari, R. *Coord. Chem. Rev.* **2005**, *249*, 525–543; (b) Bigmore, H. R.; Lawrence, C. S.; Mountford, P.; Tredget, C. S. *Dalton Trans.* **2005**, 635–651; (c) McCleverty, J. A.; Meyer, T. J. *Comprehensive Coordination Chemistry II: From Biology to Nanotechnology*; Elsevier: Amsterdam, 2003; Vol. 1; (d) Byers, P. K.; Canty, A. J.; Skelton, B. W. *Organometallics* **1990**, *9*, 826–832.
- (a) Reger, D. L.; Grattan, C. G.; Brown, K. J.; Little, C. A.; Lamba, J. J. S.; Rheingold, A. L.; Sommer, R. D. *J. Organomet. Chem.* **2000**, *607*, 120–128; (b) Kläui, W.; Berghahn, M.; Rheinwald, G.; Lang, H. *Angew. Chem., Int. Ed.* **2000**, *39*, 2464–2466; (c) Reger, D. L.; Little, C. A. *Inorg. Chem.* **2001**, *40*, 1508–1520; (d) Reger, D. L.; Semeniuc, R. F.; Little, C. A.; Smith, M. D. *Inorg. Chem.* **2006**, *45*, 7758–7769; (e) Mendez, A. S.; Ortiz, A. M.; Flores, J. C.; Sal, P. G. *Dalton Trans.* **2007**, 48, 5658–5669; (f) Bigmore, H. R.; Dubberley, S. R.; Kranenburg, M.; Lawrence, C. S.; Sealey, A. J.; Selby, J. D.; Zuideveld, M. A.; Cowley, A. R.; Mountford, P. *Chem. Commun.* **2006**, 436–438.
- (a) Alegria, E. C. B.; Martins, L. M. D. R. S.; Haukka, M.; Pombeiro, A. J. L. *Dalton Trans.* **2006**, 41, 4954–4961; (b) Alegria, E. C. B.; Martins, L. M. D. R. S.; Guedes da Silva, M. F. C.; Pombeiro, A. J. L. *J. Organomet. Chem.* **2005**, *690*, 1947–1958; (c) Wanke, R.; Smoleski, P.; Martins, L. M. D. R. S.; Guedes da Silva, M. F. C.; Pombeiro, A. J. L. *Inorg. Chem.* **2008**, *47*, 10158–10168.
- Breher, F.; Grunenberg, J.; Lawrence, C. S.; Mountford, P.; Rügger, H. *Angew. Chem., Int. Ed.* **2004**, *43*, 2521–2524.
- (a) Kuzu, I.; Kruppenacher, I.; Meyer, J.; Armbruster, F.; Breher, F. *Dalton Trans.* **2008**, 43, 5836–5865; (b) Bigmore, H. R.; Meyer, J.; Kruppenacher, I.; Rügger, H.; Clot, E.; Mountford, P.; Breher, F. *Chem.—Eur. J.* **2008**, *14*, 5918–5934; (c) Kuzu, I.; Kruppenacher, I.; Hewitt, I. J.; Lan, Y.; Mereacre, V.; Powell, A. K.; Höfer, P.; Harmer, J.; Breher, F. *Chem.—Eur. J.* **2009**, *15*, 4350–4365; (d) Kruppenacher, I.; Rügger, H.; Breher, F. *Dalton Trans.* **2006**, 8, 1073–1081; (e) Lawrence, C. S.; Skinner, M. E. G.; Green, J. C.; Mountford, P. *Chem. Commun.* **2001**, 705–706; (f) Byers, P. K.; Carr, N.; Stone, F. G. A. *Dalton Trans.* **1990**, 3701–3708; (g) Byers, P. K.; Stone, F. G. A. *Dalton Trans.* **1991**, 1, 93–99.
- (a) Janiak, C. *J. Chem. Soc., Dalton Trans.* **2000**, 21, 3885–3896; (b) Hobza, P.; Havlas, Z. *Chem. Rev.* **2000**, *100*, 4253–4264; (c) Müller-Dethlefs, K.; Hobza, P. *Chem. Rev.* **2000**, *100*, 143–167; (d) Nishio, M. *Cryst. Eng. Commun.* **2004**, *6*, 130–158.
- (a) Gamez, P.; Mooibroek, T. J.; Teat, S. J.; Reedijk, J. *Acc. Chem. Res.* **2007**, *40*, 435–444; (b) Joseph, J.; Jemmis, E. D. *J. Am. Chem. Soc.* **2007**, *129*, 4620–4632; (c) Lu, Y. X.; Zou, J. W.; Wang, Y. H.; Yu, Q. S. *Chem. Phys.* **2007**, *334*, 1–7.
- Frisch, M. J.; Trucks, G. W.; Schlegel, H. B.; Scuseria, G. E.; Robb, M. A.; Cheeseman, J. R.; Zakrzewski, V. G.; Montgomery, J. A., Jr.; Stratmann, R. E.; Burant, J. C.; Dapprich, S.; Millam, J. M.; Daniels, A. D.; Kudin, K. N.; Strain, M. C.; Farkas, O.; Tomasi, J.; Barone, V.; Cossi, M.; Cammi, R.; Mennucci, B.; Pomelli, C.; Adamo, C.; Clifford, S.; Ochterski, J.; Petersson, G. A.; Ayala, P. Y.; Cui, Q.; Morokuma, K.; Malick, D. K.; Rabuck, A. D.; Raghavachari, K.; Foresman, J. B.; Cioslowski, J.; Ortiz, J. V.; Stefanov, B. B.; Liu, G.; Liashenko, A.; Piskorz, P.; Komaromi, I.; Gomperts, R.; Martin, R. L.; Fox, D. J.; Keith, T.; Al-Laham, M. A.; Peng, C. Y.; Nanayakkara, A.; Gonzalez, C.; Challacombe, M.; Gill, P. M. W.; Johnson, B. G.; Chen, W.; Wong, M. W.; Andres, J. L.; Head-Gordon, M.; Replogle, E. S.; Pople, J. A. *Gaussian 98, Revision A.9*; Gaussian: Pittsburgh, PA, 1998.
- Becke, A. D. *J. Chem. Phys.* **1993**, *98*, 5648–5652.
- Lee, C.; Yang, W.; Parr, R. G. *Phys. Rev.* **1988**, *B37*, 785–789.
- Reed, A. E.; Curtiss, L. A.; Weinhold, F. *Chem. Rev.* **1988**, *88*, 899–926.
- (a) Sheldrick, G. M. *Acta Crystallogr., Sect. A* **1990**, *46*, 467–473; (b) Sheldrick, G. M. *SHELXL-97*; University of Gottingen: Germany, 1997; (c) Farrugia, L. J. *J. Appl. Crystallogr.* **1999**, *32*, 837–838.
- Reger, D. L.; Collins, J. E. *Organometallics* **1997**, *16*, 349–353.